Single View Augmentation of 3D Elastic Objects

Nazim Haouchine, Jérémie Dequidt, Marie-Odile Berger, Stéphane Cotin

Single View Augmentation of 3D Elastic Objects

Nazim Haouchine* Inria Lille University
Jeremie Dequidt† Lille University Inria
Marie-Odile Berger‡ Inria Lorraine University
Stephane Cotin§ Inria Lille University

ABSTRACT

This paper proposes an efficient method to capture and augment highly elastic objects from a single view. 3D shape recovery from a monocular video sequence is an underconstrained problem and many approaches have been proposed to enforce constraints and resolve the ambiguities. State-of-the art solutions enforce smoothness or geometric constraints, consider specific deformation properties such as inextensibility or ressort to shading constraints. However, few of them can handle properly large elastic deformations. We propose in this paper a real-time method which makes use of a mechanical model and is able to handle highly elastic objects. Our method is formulated as a energy minimization problem accounting for a non-linear elastic model constrained by external image points acquired from a monocular camera. This method prevents us from formulating restrictive assumptions and specific constraint terms in the minimization. The only parameter involved in the method is the Young's modulus where we show in experiments that a rough estimate of its value is sufficient to obtain a good reconstruction. Our method is compared to existing techniques with experiments conducted on computer-generated and real data that show the effectiveness of our approach. Experiments in the context of minimally invasive liver surgery are also provided.

Index Terms: H.5.1 [Information Interfaces and Presentation]: Multimedia Information Systems—Artificial, augmented, and virtual realities; I.3.5 [Computer Graphics]: Computational Geometry and Object Modeling—Physically based modeling

1 INTRODUCTION

3D recovery and augmentation of deformable objects in a monocular context is a challenging problem with many potential applications in computer graphics, augmented reality and medical imaging. The difficulties originate from the fact that the problem is underconstrained. To overcome this problem, various approaches have been considered with the aim to provide additional contraints and solve the ambiguities. Many approaches introduced deformation models which are often learned from training data and derive models with few degrees of freedom. A lot of papers have been devoted to inelastic materiels such as papers, sails, clothes ... and make use of the inextensibilty constraint, ensuring that the distance between points remains constant. Other geometric or shading constraints have been proposed to handle materials that can stretch. However, the additional constraints that are used are not always suited to the properties of the object. That is the reason why we advocate in this paper the use of a mechanical model within a non-linear elasticity framework to enable reconstruction and augmentation of highly deformable objects. Our model only requires the knowledge of the Young's modulus. Mechanical models have been seldom used in the past due the difficulty to acquire the parameters of the model and the complexity of non-linear models which precludes real time algorithms. In this paper, we propose an efficient real-time algorithm for recovery and augmentation of highly elastic objects in a monocular context. We also show that a rough estimation of the Young's modulus is sufficient to obtain a good reconstruction while imposing sufficient boundary constraints. Applications of the method are provided in the context of augmented reality for minimally invasive liver surgery. Augmented Reality techniques are considered as a well-suited approach in order to enrich visual feedback of surgeons during minimally invasive procedures [18] where surgeons do not directly manipulate the organ but interact with the organ using instruments inserted through small incisions around the abdominal cavity. Visualization of additional pre-operative information - such as tumors- in the field of view of the surgeon requires to track in real time possibly large elastic deformations of the liver. Existing techniques that take into account organ elasticity [11] [23] have been proposed. These methods rely on a combination of a stereo estimation of organ motion and on biomechanical models to characterize the elastic behaviour. Despite the fact that these methods yield good results, stereo-laparoscopic cameras are uncommon compared to mono–laparoscopic camera (less than 1%), which motivated us to investigate this limitation.

Figure 1: Three-dimensional reconstruction and augmentation of elastic objects from a single view under several elongations. Our approach is able to handle extensibility of the material when undergoing elongation. In (top) the camera view of the re-textured elastic object and in (bottom) the recovered 3D shape form showed from a different view.

The paper is organized as follows. Existing techniques for 3D recovery of elastic objects are presented in Section 2. Our method is explained in Section 3, 4 and 5. The obtained results are exposed in Section 6 and show that the method is able to cope with large elastic deformation in a various dataset including surgery data.

*e-mail: nazim.haouchine@inria.fr
†e-mail: jeremie.dequidt@inria.fr
‡e-mail: marie-odile.berger@inria.fr
§e-mail: stephane.cotin@inria.fr

2 Related works and Contribution

In the early works on augmented reality for deformable objects, registration of images of a deforming surface was obtained by computing dense 2D/2D transformations using points correspondences. A parametric representation of the deformation or regularization techniques were needed to prevent excessive wrinkling of the surface in the presence of erroneous correspondences. In [4], Bartoli et al. take advantage of a rich texture information to perform points matching between images, allowing a 2D deformation motion model to be computed using Radial Basis Mapping. Pilet *et al.* [21] proposed a template-based fast and robust tracking for handling deformations. This approach uses a set of wide baseline feature matches assuming a well textured surface and combines 2D deformable meshes with a robust estimation technique. Zhu *et al.* [34] demonstrate that a Finite Newton algorithm and an efficient factorization method can reduce the number of iterations of the previous method to solve the optimization problem. In order to handle the more challenginging case of deformation with self occlusions, Gay-Belille *et al.* [8] considered the occluded pixels as self-occlusion area that forces the wrap to shrink instead of outliers. Inspired by this self-occlusion shrinking method, Hilsmann *et al.* [12] proposed an approach exploiting an optical flow extended by a specific illumination model which jointly estimates deformation and illumination and can cope with self-occlusions through an occlusion map computed from local statistical color models. In [22], self occlusions are detected as outliers based on the assumption that the surface to detect is locally smooth.

However, these methods based on 2D images transformations are well suited to smooth deformations but are not suitable for highly elastic objects. In fact, elastic deformations in the 3D space can lead to highly complex 2D deformations in the image plane, especially due to self occlusions, making inappropriate the use of regularization contraints. For these reasons, state-of-the art methods perform 3D reconstruction of deformable surfaces in a monocular context since elasticity constraints are often known or can be expressed in a more natural way on the 3D objets. Recovering the 3D shape of a deformable surface from a monocular video and a template (a *reference* image of the surface for which the 3D shape is known) can be ambiguous. Therefore additional consistency constraints are required to solve ambiguities. The inextensibility constraint is widely used to recover and augment objets as sheets of paper, sails, tee-shirts... [27, 19]. Methods differ in the way inextensibility is considered as a hard constraint or a penalty term and also in the efficiency of the convex or non-convex optimization associated to the procedure. In the general case, global smoothness constraints are common to resolve the ambiguities of 3D reconstruction. Many papers ressort to a linear description of feasable object deformation. Most of the time, it is generated from a representative sample of possible shapes using a dimensionality reduction process [26, 24].

Some works attempt to overcome the need to provide plausible constraints on the deformation by using richer sources of information. In [16] a closed-form solution constrained by shading informations was introduced to capture stretching surface. This method assumes a Lambertian surface with a single point light source and yield good results. However, the strong assumptions on the lighting make the method hard to generalize in all environments. Other methods have been designed to cope with non smooth deformations, as folding. Salzmann *et al.* [25] propose to solve the problem as a convex minimization of the reprojection error formulated as a Second Order Cone Programming (SOCP). The method restricts the motion from one frame to the next but do not impose unwarranted surface smoothness, making it possible to recover sharp folds.

Recently, many examples of mechanical-based tracking methods have emerged. For instance the approach in [1], where a combination of Finite Element Modelling with and Extended Kalman Filter shows the efficiency of physics-based method. In [31], a linear finite element method is used to predict the deformation. The approach described in [14] relies on the minimization of a stretching energy subject to external image constraints. The problem is formalized as a non-linear minimization that unifies geometric constraints assuming a projective camera and mechanical constraints assuming local linear elasticity. This method shows effective results but is however limited to compressible objects by considering the Poisson ratio as the unique mechanical parameter.

Contribution

The main contribution of this paper is to provide an efficient method to capture and augment a 3D elastic surface from a single viewpoint. By assuming a prior knowledge of the material elasticity (represented by the Young's modulus), large strains of more than 130% can be efficiently handled. To the best of our knowledge, no similar method has been proposed in the case of monocular camera.

3 Non Linear Elastic model

The choice of a relevant constitutive model is essential as it will determine the set of deformations we are able to capture and estimate while discriminating non-plausible material configurations induced by tracking errors. Two important assumptions are also made in order to reduce the complexity of the deformation model and the number of related parameters. First, the material of the deformable object will be *homogeneous* meaning that a uniform deformation will lead to equal (in magnitude) forces for any points of the object. Second, the material will also considered as *isotropic* meaning that the response to a deformation is independent of the orientation of the deformation. Moreover computation time is also a key constraint as the targeted application should be *interactive*. Interactive (or at least computationally fast) models for deformable solids have been a major topic in the computer graphics community. Several reports or surveys have been published to provide an exhaustive overview of state-of-the-art methods [9, 17, 28]. In that context, Saint Venant-Kirchhoff model [28] appears to be an ideal compromise because it is able to handle non-linear deformations, is rotationally invariant and is simple enough compared to other non-linear model and therefore can be computed at interactive rates. Several downsides however exists such as incorrect stress estimation under extreme compression and sometimes the requirement to use non-linear solvers to compute the motion over time. Incorrect stress estimation under any large deformations is not a major issue in our context since we are interested in capturing an accurate deformation field and since the stress field is not measurable with camera images. Recent works in simulation or in haptics rendering have proposed computationally fast non-linear solvers such as [29] which leverages the pre-requisites of use non-linear solvers with Saint Venant-Kirchhoff model.

A Saint Venant-Kirchhoff (StVK) material is a material for which the Green-Lagrange strain tensor $\mathbf{E} \in \mathbb{R}^{3x3}$ is computed as a non-linear (quadratic) function of the deformation gradient $\mathbf{F} \in \mathbb{R}^{3x3}$ as:

$$\mathbf{E} = \frac{1}{2}(\mathbf{F}^T\mathbf{F} - \mathbf{I}) \tag{1}$$

where $\mathbf{I} \in \mathbb{R}^{3x3}$ is the identity matrix. The computation of the strain tensor maybe computationnaly intensive and several approaches have been investigated for interactive uses. For instance, Barbic and James [2] uses model reduction and pre-computation reduced coordinates while Zhong *et. al.* [33] uses pre-computed relation between surface and internal nodes. In this paper, the elegant approach of Kikuuwe *et. al.* [13] is chosen since it does not require pre-computation nor does it make any assumption of the deformations that will be generated. To do that, fast computation is conducted using dedicated yet simple data-structures (tetrahedron-sharing edge-pairs). We will detail the main points of Kikuuwe *et.*

al. but we encourage the reader to refer to [13] for complete analysis and implementation details. If v is a point in the deforming medium and v_0 is its initial location, $\mathbf{F}$ can be expressed as $\mathbf{F} = \frac{\partial v}{\partial v_0}$ Since $\mathbf{E}$ is symmetric, its form is as follows:

$$\mathbf{E} = \begin{bmatrix} \varepsilon_{xx} & \varepsilon_{xy} & \varepsilon_{zx} \\ \varepsilon_{xy} & \varepsilon_{yy} & \varepsilon_{yz} \\ \varepsilon_{zx} & \varepsilon_{yz} & \varepsilon_{zz} \end{bmatrix} \tag{2}$$

and the 6 independent coefficients may be placed in a single vector ε using Voigt notation:

$$\varepsilon = [\varepsilon_{xx}, \varepsilon_{yy}, \varepsilon_{zz}, 2\varepsilon_{xz}, 2\varepsilon_{yz}, 2\varepsilon_{zx}]^T \tag{3}$$

Computing $\mathbf{E}$ is often conducted by using a strain energy density w that will be integrated over the whole deforming medium X through the following equation:

$$\mathbf{E} = \int_X w \, dX \tag{4}$$

An isotropic homogeneous Saint Venant-Kirchhoff material has w expressed with the following equation:

$$w = \varepsilon^T \, \mathbf{D} \, \varepsilon / 2 \tag{5}$$

where $\mathbf{D} \in \mathbb{R}^{6x6}$ is the following matrix:

$$\mathbf{D} = \begin{bmatrix} \lambda+2\mu & \lambda & \lambda & 0 & 0 & 0 \\ \lambda & \lambda+2\mu & \lambda & 0 & 0 & 0 \\ \lambda & \lambda & \lambda+2\mu & 0 & 0 & 0 \\ 0 & 0 & 0 & \mu & 0 & 0 \\ 0 & 0 & 0 & 0 & \mu & 0 \\ 0 & 0 & 0 & 0 & 0 & \mu \end{bmatrix} \tag{6}$$

where λ and μ are *Lamé* coefficients and can be computed thanks to the elastic parameters of the material E and ν. E is the Young's modulus and is a measure of the stiffness of the material while ν is the Poisson's ratio and estimates the compressibility of the material.

For a deforming medium of arbitrary shape, it is often convenient to discretize the shape using elementary and simple elements. Tetrahedral decomposition is often considered since efficient meshing algorithms exist[1]. For a tetrahedron t, let us consider the edge e among the 6 possibles edges of t, e being connected two vertices v_i and v_j. Be $l_e = v_i - v_j$ and $l_e^0 = v_i^0 - v_j^0$. Assuming that the deformation gradient $\mathbf{F}$ is constant in the neighbor of t and has the value $\mathbf{F}_t$, l_e can be estimated as $F_t l_e$. The equation (1) can be used to write:

$$\begin{array}{rcl} l_e^T \mathbf{E}_t l_e & = & \frac{1}{2} l_e^T (\mathbf{F}_t^T \mathbf{F}_t - I) l_e \\ l_e^T \mathbf{E}_t l_e & = & \frac{1}{2} (\|l_e\|^2 - \|l_e^0\|^2) \end{array} \tag{7}$$

l_e^0 can also be written in Voigt notation using the variable q_e^0 defined as:

$$q_e^0 = \begin{bmatrix} (v_i.x - v_j.x)^2 \\ (v_i.y - v_j.y)^2 \\ (v_i.z - v_j.z)^2 \\ (v_i.x - v_j.x)(v_i.y - v_j.y) \\ (v_i.y - v_j.y)(v_i.z - v_j.z) \\ (v_i.z - v_j.z)(v_i.x - p_j.x) \end{bmatrix} \tag{8}$$

[1] for instance CGAL library http://www.cgal.org

where for each value $.x$, $.y$, $.z$ is the first / second / third component of the considered vector. The previous equation is the rewritten by using Voigt notations as:

$$q_e^{0T} \varepsilon_t = \frac{1}{2} (\|l_e\|^2 - \|l_e^0\|^2) \tag{9}$$

This equation is considered for a single edge e but is suitable for the other edges. By considering the 6 edges of the tetrahedron t, we obtain the following equation:

$$\mathbb{Q}_t \varepsilon_t = \frac{1}{2} \mathbb{L}_t \tag{10}$$

where $\mathbb{Q}_t = [q_0^0, q_1^0, q_2^0, q_3^0, q_4^0, q_5^0]^T$ (q_e for the 6 possibles edges) and $\mathbb{L}_t = [\|l_0\|^2 - \|l_0^0\|^2, \|l_1\|^2 - \|l_1^0\|^2, \ldots]^T$ (again for the 6 possible edges). It should be noted that $\mathbb{Q}_t \in \mathbb{R}^{6x6}$ and $\mathbb{L}_t \in \mathbb{R}^6$. $\mathbb{Q}_t$ is invertible if the 4 points are not linearly dependent and therefore ε_t can be estimated as:

$$\varepsilon_t = \frac{1}{2} \mathbb{Q}_t^{-1} \mathbb{L}_t \tag{11}$$

enabling to compute the strain energy in the tetrahedron t with

$$W_t = \varepsilon_t^T \, \mathbf{D} \, \varepsilon_t / 2 \tag{12}$$

Therefore the total strain energy $W = \sum W_t$ of the medium as a function of the edge lengths of the tetrahedral mesh and elastic parameters. Eventually the forces exerted on the vertices can be computed as:

$$f(v) = \frac{\partial W}{\partial v^T} \tag{13}$$

For computation purposes, a global stiffness matrix is also computed as:

$$K(v) = \frac{\partial f(v)}{\partial v} \tag{14}$$

as it allows for a displacement dv (such as $v' = v + dv$) of the vertices of the mesh to compute the resulting forces as:

$$f(v) = K(v) \times dv \tag{15}$$

This is a convenient equation that relates forces to any displacement of the vertices but again it should be reminded that the matrix $K(v)$ should be recomputed after every deformation to remain valid.

4 Problem Formulation

The non-rigid surface reconstruction from a single view can be formalized as the minimization of a reprojection error. By assuming a known and constant projection matrix P, the projection of a point $M = (X, Y, Z)$ in the image is given by:

$$m = \begin{pmatrix} x \\ y \end{pmatrix} = PM = \begin{pmatrix} \frac{P_{11}X + P_{12}Y + P_{13}Z + P_{14}}{P_{31}X + P_{32}Y + P_{33}Z + P_{34}} \\ \frac{P_{21}X + P_{22}Y + P_{23}Z + P_{24}}{P_{31}X + P_{32}Y + P_{33}Z + P_{34}} \end{pmatrix} = \begin{pmatrix} \frac{P_1 M}{P_3 M} \\ \frac{P_2 M}{P_3 M} \end{pmatrix} \tag{16}$$

where P_k is the k^{th} row of the projection matrix P.

For a set of n point, minimizing the reprojection error with respect to the point $\hat{m} = (\hat{x}, \hat{y})$ that correspond to the projection of M in the image amount to minimize the quantity:

$$\sum_{i=1}^{n} \left\| \frac{P_1 M_i}{P_3 M_i} - \hat{x}_i, \frac{P_2 M_i}{P_3 M_i} - \hat{y}_i \right\| \tag{17}$$

In practice, additional penalties functions are used to obtain a well-constrained system. This constraints are often based on the inextensibility property of the surface to be recovered. Since such constraints cannot be considered in our case, we propose to consider

the elastic registration as a stretching energy minimization problem that accounts for the internal forces of the mechanical and external forces emanated from the visual tracking. We here assume that the following data are available:

- The projective matrix P assuming orthographic projection.
- The correct initial alignment of the mesh (in rest configuration) on the image.
- A set T of paired point between the set of features $U = \{u_i \in \mathbb{R}^2\}$ from visual tracking and the vertices of the mesh $V = \{v_i \in \mathbb{R}^3\}$ related to the mechanical model.
- The Young's modulus E that represent the elasticity of the mechanical model.

At initialization each feature u_i is associated with a 3D point $\hat{u}_i$ by intersection the line of sight with the surface. $\hat{u}_i$ is expressed as a barycentric combinaison of the neighbouring vertices N_i of the mesh: $\hat{u}_i = \sum_{j \in N_i} \gamma_{ij} v_j$. We assume that this linear relation remains valid during the deformation. At any later time, the stretching energy induced by the visual tracking is defined as:

$$\sum_{i \in T} \frac{1}{2} \alpha \| v_i - P(\hat{u}_i) \|^2 \tag{18}$$

where α can be seen as a stiffness and is experimentally chosen to at the same order of magnitude of the Young's modulus. In order to obtain a system that is sufficiently constrained to give good results, we add to the system a set B of boundary constraints by using the term:

$$v_i = Q_i \; for \; i \in B \tag{19}$$

where Q_i is the known boundary conditions that can be seen as a set of fixed vertices. The minimization problem is then formulated as a constrained minimization between internal elastic energy and stretching energy and can be written as follows:

$$\begin{array}{ll} minE(v) & = \sum_t W_t + \sum_{i \in T} \frac{1}{2} \alpha \| v_i - P(\hat{u}_i) \|^2 \\ subject\ to & v_i = Q_i \; for \; i \in B \end{array} \tag{20}$$

where W_t is the strain energy of a tetraherdon related to a Saint Venant-Kirchhoff material and which is depending on the position of the vertices. The expression of W_t is detailed in the equation (12).

5 Resolution

The equation (20) is a classical constrained minimization problem. We choose to solve this equation by formulation a linear complementary problem (LCP) that will be solved with a Gauss-Seidel algorithm using the approach in [10]. Finding the minimum of energy is conducted by deriving and setting to zero the equation (20). This leads to an equality between internal elastic forces and stretching forces and this is equivalent of finding the equilibrium state of the material due to external forces. Indeed kinetic energy is not considered since we are not interesting in capturing transient motions because first, the materials used are very soft and second, the acquisition rate is high enough; therefore the deformation exhibit no significant transient motion. The method proposed in [10] is a two-steps solver that is able to find a constrained minimum by considering first a free-motion and second applying a corrective motion to satisfy our boundary conditions. The reader may refer to [10] for implementation details. Even if our approach is static (without dynamic due to kinetic energy of the material), it can easily be adapted to dynamic motion with the same method by adding a non-linear differential equation solver such as an implicit Euler with a conjugate gradient [7].

6 Experimental Results

In this section we present the results obtained using our method and the comparison conducted with existing techniques. We report results obtained on three type of data: Silicone-made data, computer-generated data and liver data during *in-vivo* surgical procedure. To test the ability of our approach to capture 3D elastic deformations, we capture several video sequences of a silicone-like object undergoing different type of stretching deformation. We quantify the three-dimensional shape recovery error with respect to a ground truth while visual assessment is reported on surgical data. We use the SURF [5] for image point correspondence where the number of detected point can be easily tuned. Note that other descriptors can easily been plugged to the framework and take advantage of recent work on vision-based tracking of living tissue [32].

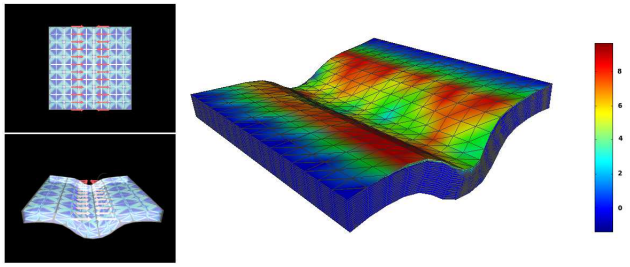

(a)

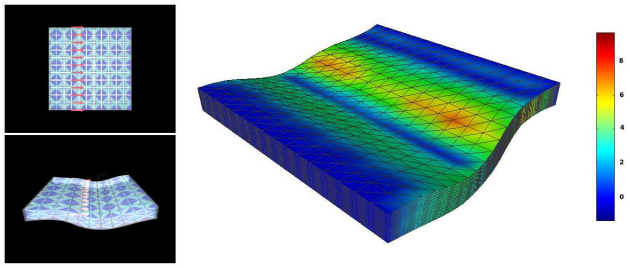

(b)

Figure 2: 3D registration error on two computer-generated sequences. The applied forces are represented with red arrows and the tetrahedral elements in blue, for (a) simulation 1 where two forces in opposite directions are applied and (b) simulation 2 where a single force is applied.

6.1 Computer-generated Data

We used the framework Sofa [7] to generate elastic deformations of a silicone-like object with a Young's Modulus of $E = 0.25$ MPa. A force F is applied on the object to produce a 3D deformation (cf Figure 2). A video sequence of the deformations is captured with a virtual camera (diag(500,500,1)). The external stifness parameter is set to be equal to the synthetic force $\alpha = F$. The Figure 2 illustrate the results obtained by calculating the Hausdorff Distance between the tracked and simulated mesh where we report an average error of 3.16 mm for the simulation 1 and 2.90 mm for the simulation 2.

We also conduct experiments on the same set of data where we vary the Young's Modulus value. The plot 3 shows that small variation of E slightly affect the registration error in comparison with the large errors that produce greater or lower values. In the mean time, we notice that a value of α close to the Young's Modulus gives the best results in term of accuracy.

It should be emphasized that a further sensitivity study is required to identify the most influential parameters of the simulation. The conducted experiments only highlight that an approxi-

mate value of the Young's Modulus is enough to yield convincing registration results. In fact, depending on the way the constraints on the deformable structure are modeled, the resulting deformation can be entirely independent of the Young's Modulus. The reader may refer to [15] for a more detailed study on the impact of material properties when dealing with soft-tissue simulation.

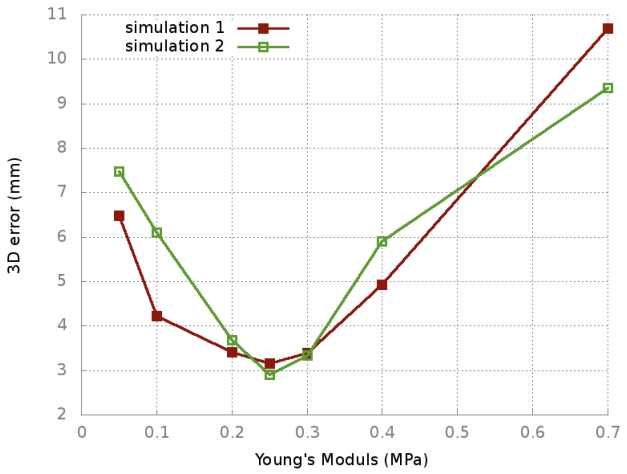

Figure 3: 3D registration error on with variation of the Young's Modulus for simulation 1 and simulation 2: Small variation of the Young's Modulus value slightly affect the reconstruction while distant values highly increase the errors.

6.2 Real Data

We test our method on a silicone-like object with a size of $100 \times 100 \times 10$ mm^3 composed of linear P1 tetrahedral elements characterized by a Young's Modulus $E = 0.25$ MPa. The image are acquired with a monocular camera at 30 fps with an image resolution of 640×480. The implementation is done in C++ on a PC with and Intel i7 M620 2.76GHz processor.

6.2.1 2D Surface Registration and Retexturing

The aim of conducting tests on 2D surface is to be able to measure the registration error w.r.t the deformation of the object. Since the boundaries of the object can be easily extracted in the image, a way to quantify this error is to compute the distance beween the silhouette computed from the recovered 3D object and the actual boundaries extracted in the image. The results reported in the plot 4 gives the small 2D error even when the elongation increases (more than 120%). The relation between the accuracy of the augmentation and the number of tetrahedron elements is also reported in figure 4 where we can notice that a finer mesh resolution reduce the registration error.

In order to ensure real-time achievement, a compromise has to be found between the number of elements and the computation time. While a large number of elements permits to obtain an accurate registration, it also increases the computation time. The Table 6.2.1 gives the average errors and computation time w.r.t the mesh resolution.

Table 1: Impact of the number of elements on the computation time.

Number of elements	256	**576**	1024	1600
Average 2D Error (px)	27.66	**18.55**	17.61	16.72
Frame rate (fps)	29	**17**	9	5

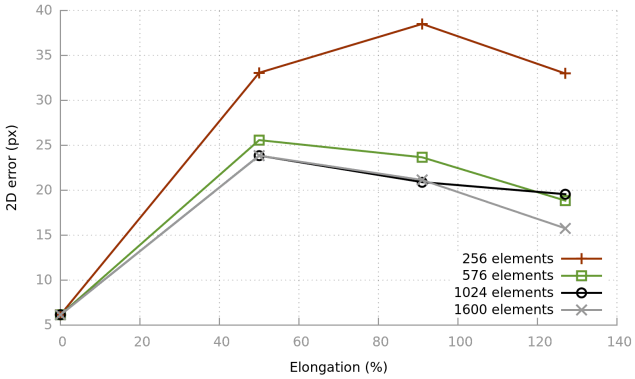

Figure 4: Registration error with respect to object elongation with a variation of mesh resolution: With an adequate number of tetrahedral elements the projection error can be significantly reduced.

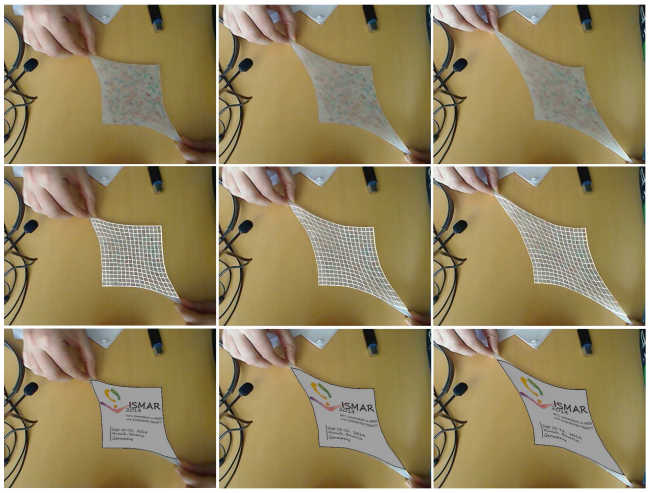

Figure 5: Selected frames during a 2D elastic surface augmentation of the silicone-like material when being stretched up to 120%, with (top) input images (middle) registered mesh (bottom) surface retexturing.

6.2.2 3D Shape Recovery and Augmentation

For the three-dimensional reconstruction we propose to test our approach on 4 types of deformations, with extensibility up to 130% as illustrated in Figure 6. We calculate the euclidean distance between the reconstructed surface and a ground truth obtained with Structure from Motion techniques [30]. We compare our method with 3 existing approaches: a template-based method for isometric and conformal surface reconstruction described in [3] the code of which is freely available, a classic mass-spring model and a mechanical-based approach that considers a linear Strain/Stress formulation [6]. The plots and the resulting shapes are illustrated in Figure 7.

Deformation 1: By stretching the object with an elongation of 30%, we force the surface to fold. The linear FEM and the template-based approach fail to correctly recover the 3D shape. The non-linear method gives the lowest error with 2.62 mm with only 26 detected features.

Deformation 2: The surface is constrained with a rigid beam and stretched to produce a triangle-like shape. Only the mass-spring

models was not able to recover the deformation. The template-based approach yields good results. However, the mechanical methods report the more accurate registration with very close error: 2.52 mm for the Linear FEM and 2.44 mm for out method. The number of features extracted is 28 for all the methods except the template-based where 237 features are necessary to yield good results.

Deformation 3: The object is elongated down and constrained at the center of the object. The four methods succeed to recover the the shape deformation with 174 extracted features. Our method outperforms the others with an error of 2.06 mm.

Deformation 4: Our approach gives the smallest error with 1.69 mm where the extensibility is about 130%. The object highly elongated during the deformation and produces a 3D shape by partially folding. The template-based method fails to recover the stretched shape while the mass-spring and linear FEM models give relatively good shape representations.

6.3 Surgical data

Our aim is to assess the robustness of our approach in a real environment (specular lights, beating heart, respiratory motion, instrument occlusions) and the ability of our non-rigid registration in recovering 3D shapes from a single view. In our past works on liver augmentation [11], we mainly consider deformations of the liver that mainly occurs in a fronto-parallel plane but not very in depth. In addition, visual features were acquired in 3D thanks to a stereo-vision set-up. Here a general motion of the liver is considered, with possible folds, in the monocular context which is a much more complex situation. We test our approach on an video of *in-vivo* porcine liver showing one of the liver lobe undergoing elastic deformation during a minimally invasive surgery. We used a monocular laparoscopic camera from Karl Storz Endoscopy acquiring video stream in 25 FPS with image resolution of 720×576 pixels and data computed from pre-operative scans. This data permits to generate the necessary mesh for a correct modelling of the liver in three steps: segmentation, volume generation and parametrisation.

Segmentation: The volume issued from CT-scanner is used to generate the liver surface. This segmentation is done semi-manually using active contour techniques (Snake) using the software itksnap [2].

Volumetric mesh generation: Volumetric mesh are necessary for a finite element modelling. To generate this volume from surface we use CGal library. The number of elements is to be chosen carefully in order to ensure real-time performance as long as sufficient accuracy.

Parametrisation: The elastic parameter (Young's modulus) is set according to [20] to E=27 KPa with a model composed of 3914 linear P1 tetrahedral elements.

These steps are commonly performed before a surgical procedure which permit to our framework to easily take advantages of the data. The Young's modulus is extracted from a textbook and does not suit exactly the considered liver. The results illustrated in the Figure 8 report a visually correct 3D elastic augmentation of the liver model on the laparoscopic image with a good 3D shape recovery.

7 Conclusion

In this paper, we have proposed a real time and efficient method to capture and augment highly elastic objects from a single view. This method makes use of a mechanical model of the deformable object in the context of non linear elasticity. With respect to many existing approaches, this method makes it possible to avoid the definition of adhoc constraints to solve the ambiguities of reconstruction. Experiments conducted in the paper prove that the method is flexible in the sense that a classical model - the St Venant-Kirchhoff model- has proven to be sufficient to handle various applications with a good accuracy. The orthographic projection is currently used in our method in the image term since the minimization is easier than with the perspective projection. Integration of a fully perspective model will be done in the very near future. Moreover, handling partial and self-occlusions is also one axe of future development since our experiments highlight that a few number of image point are sufficient to yield good results.

[2] http://www.itksnap.org

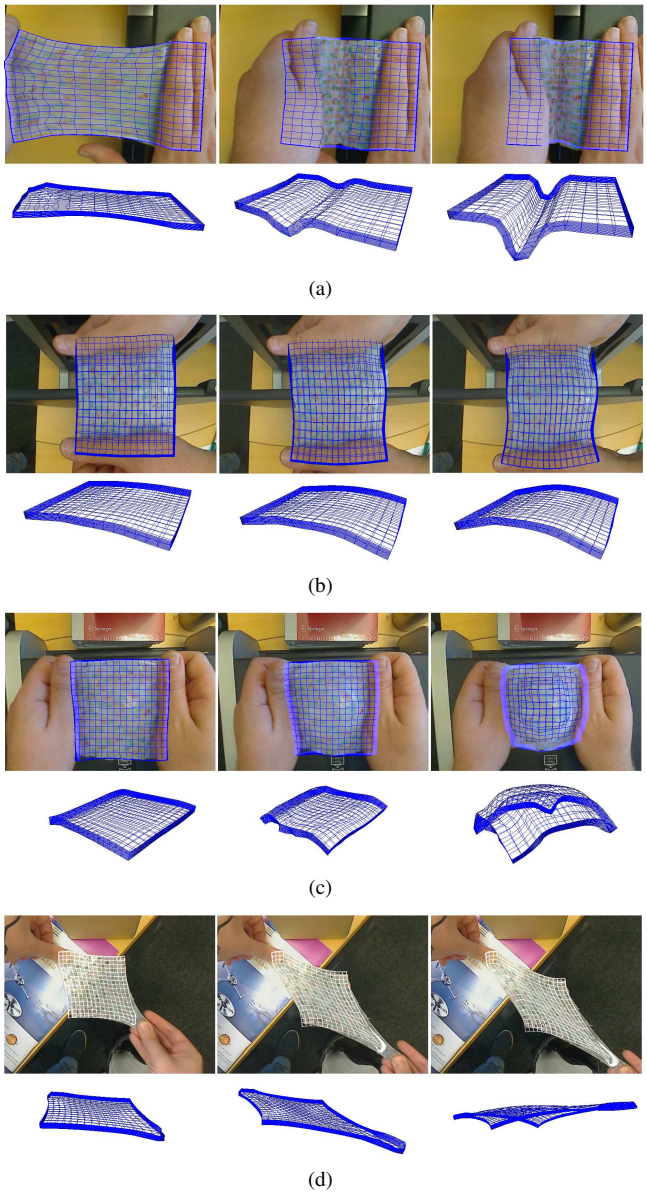

Figure 6: Selected frames showing the overlay of the mesh on the images with the silicone-like data with (a) deformations 1, (b) deformation 2 (c) deformation 3 and (d) deformations 4.

References

[1] A. Agudo, B. Calvo, and J. M. M. Montiel. Finite element based sequential bayesian non-rigid structure from motion. In *Computer Vision and Pattern Recognition, 2012. CVPR'12. IEEE Conference on*, pages 1418–1425, 2012.

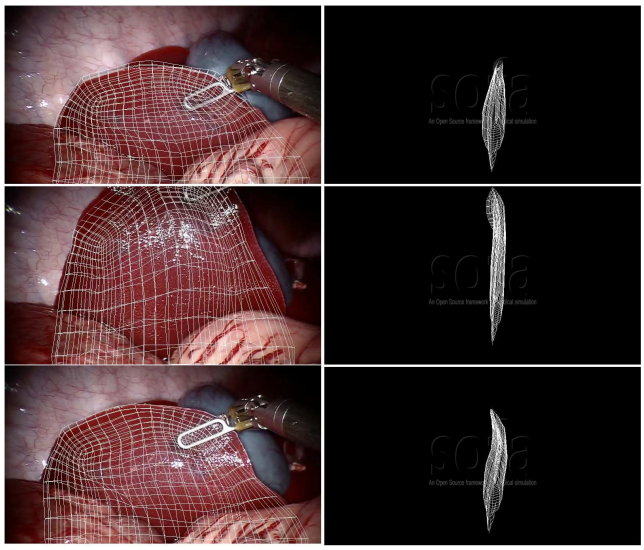

Figure 8: 3D elastic augmentation of the mechanical model on the laparoscopic images acquired form a monocular camera. The augmentation is effective (left) even when the deformation generated by the instrument force the lobe of the liver to fold (right).

[2] J. Barbič and D. L. James. Real-time subspace integration for st. venant-kirchhoff deformable models. In *ACM Transactions on Graphics (TOG)*, volume 24(3), pages 982–990. ACM, 2005.

[3] A. Bartoli, Y. Gerard, F. Chadebecq, and T. Collins. On template-based reconstruction from a single view: Analytical solutions and proofs of well-posedness for developable, isometric and conformal surfaces. In *Computer Vision and Pattern Recognition (CVPR), 2012 IEEE Conference on*, pages 2026–2033, June 2012.

[4] A. Bartoli and A. Zisserman. Direct estimation of non-rigid registration. In *In British Machine Vision Conference*, 2004.

[5] H. Bay, A. Ess, T. Tuytelaars, and L. Van Gool. Speeded-up robust features (SURF). *Comput. Vis. Image Underst.*, 110(3):346–359, June 2008.

[6] S. Cotin, H. Delingette, and N. Ayache. Real-time elastic deformations of soft tissues for surgery simulation. *Visualization and Computer Graphics, IEEE Transactions on*, 5(1):62–73, Jan 1999.

[7] F. Faure, C. Duriez, H. Delingette, J. Allard, B. Gilles, S. Marchesseau, H. Talbot, H. Courtecuisse, G. Bousquet, I. Peterlik, and S. Cotin. SOFA: A Multi-Model Framework for Interactive Physical Simulation. In Y. Payan, editor, *Soft Tissue Biomechanical Modeling for Computer Assisted Surgery*. Springer, June 2012.

[8] V. Gay-Bellile, A. Bartoli, and P. Sayd. Direct estimation of nonrigid registrations with image-based self-occlusion reasoning. *IEEE Trans. Pattern Anal. Mach. Intell.*, 32(1):87–104, Jan. 2010.

[9] S. F. Gibson and B. Mirtich. A survey of deformable modeling in computer graphics. Technical report, Mitsubishi Electronic Research Laboratory, 1997.

[10] C. Guébert, C. Duriez, and L. Grisoni. Unified processing of constraints for interactive simulation. In M. T. François Faure, editor, *Workshop in Virtual Reality Interactions and Physical Simulation VRIPHYS' 2008*, pages –, Grenoble, France, 2008. Eurographics association.

[11] N. Haouchine, J. Dequidt, I. Peterlik, E. Kerrien, M.-O. Berger, and S. Cotin. Image-guided simulation of heterogeneous tissue deformation for augmented reality during hepatic surgery. In *Mixed and Augmented Reality (ISMAR), 2013 IEEE International Symposium on*, pages 199–208, Oct 2013.

[12] A. Hilsmann, D. C. Schneider, and P. Eisert. Realistic cloth augmentation in single view video under occlusions. *Comput. Graph.*, 34(5):567–574, Oct. 2010.

[13] R. Kikuuwe, H. Tabuchi, and M. Yamamoto. An edge-based computationally efficient formulation of saint venant-kirchhoff tetrahedral finite elements. *ACM Transactions on Graphics (TOG)*, 28(1):8, 2009.

[14] A. Malti, R. Hartley, A. Bartoli, and J.-H. Kim. Monocular template-based 3d reconstruction of extensible surfaces with local linear elasticity. In *Computer Vision and Pattern Recognition (CVPR), 2013 IEEE Conference on*, pages 1522–1529, 2013.

[15] K. Miller and J. Lu. On the prospect of patient-specific biomechanics without patient-specific properties of tissues. *Journal of the Mechanical Behavior of Biomedical Materials*, 27(0):154 – 166, 2013.

[16] F. Moreno-Noguer, M. Salzmann, V. Lepetit, and P. Fua. Capturing 3d stretchable surfaces from single images in closed form. In *Computer Vision and Pattern Recognition, 2009. CVPR 2009. IEEE Conference on*, pages 1842–1849, June 2009.

[17] A. Nealen, M. Müller, R. Keiser, E. Boxerman, and M. Carlson. Physically based deformable models in computer graphics. In *Computer Graphics Forum*, volume 25 (4), pages 809–836, 2006.

[18] S. Nicolau, L. Soler, D. Mutter, and J. Marescaux. Augmented reality in laparoscopic surgical oncology. *Surgical Oncology*, 20(3):189 – 201, 2011.

[19] M. Perriollat, R. Hartley, and A. Bartoli. Monocular template-based reconstruction of inextensible surfaces. *International Journal of Computer Vision*, 95(2):124–137, 2011.

[20] I. Peterlík, C. Duriez, and S. Cotin. Modeling and real-time simulation of a vascularized liver tissue. In *Medical Image Computing and Computer-Assisted Intervention*, pages 50–57. Springer-Verlag, 2012.

[21] J. Pilet, V. Lepetit, and P. Fua. Fast non-rigid surface detection, registration and realistic augmentation. *Int. J. Comput. Vision*, 76(2):109–122, Feb. 2008.

[22] D. Pizarro and A. Bartoli. Feature-based deformable surface detection with self-occlusion reasoning. *International Journal of Computer Vision*, 97(1):54–70, 2012.

[23] P. Pratt, D. Stoyanov, M. Visentini-Scarzanella, and G.-Z. Yang. Dynamic guidance for robotic surgery using image-constrained biomechanical models. In *Medical Image Computing and Computer-Assisted Intervention*, volume 6361, pages 77–85. 2010.

[24] M. Salzmann and P. Fua. Linear local models for monocular reconstruction of deformable surfaces. *Pattern Analysis and Machine Intelligence, IEEE Transactions on*, 33(5):931–944, May 2011.

[25] M. Salzmann, R. Hartley, and P. Fua. Convex optimization for deformable surface 3-d tracking. In *Computer Vision, 2007. ICCV 2007. IEEE 11th International Conference on*, pages 1–8, Oct 2007.

[26] M. Salzmann, J. Pilet, S. Ilic, and P. Fua. Surface deformation models for nonrigid 3d shape recovery. *IEEE Trans. Pattern Anal. Mach. Intell.*, 29(8):1481–1487, Aug. 2007.

[27] S. Shen, W. Shi, and Y. Liu. Monocular 3-d tracking of inextensible deformable surfaces under l2-norm. *Trans. Img. Proc.*, 19(2):512–521, Feb. 2010.

[28] E. Sifakis and J. Barbic. Fem simulation of 3d deformable solids: A practitioner's guide to theory, discretization and model reduction. In *ACM SIGGRAPH 2012 Courses*, SIGGRAPH '12, pages 20:1–20:50, New York, NY, USA, 2012. ACM.

[29] M. Silcowitz-Hansen, S. Niebe, and K. Erleben. A nonsmooth nonlinear conjugate gradient method for interactive contact force problems. *Vis. Comput.*, 26(6-8):893–901, June 2010.

[30] N. Snavely, S. M. Seitz, and R. Szeliski. Photo tourism: Exploring photo collections in 3d. In *ACM SIGGRAPH 2006 Papers*, SIGGRAPH '06, pages 835–846, New York, NY, USA, 2006. ACM.

[31] S. Wuhrer, J. Lang, and C. Shu. Tracking complete deformable objects with finite elements. In *3DIMPVT*, pages 1–8. IEEE, 2012.

[32] M. C. Yip, D. G. Lowe, S. E. Salcudean, R. N. Rohling, and C. Y. Nguan. Tissue tracking and registration for image-guided surgery. *Medical Imaging, IEEE Transactions on*, 31(11):2169–2182, Nov 2012.

[33] H. Zhong, M. P. Wachowiak, and T. M. Peters. A real time finite element based tissue simulation method incorporating nonlinear elastic behavior. *Computer Methods in Biomechanics and Biomedical Engineering*, 8(3):177–189, 2005.

[34] J. Zhu and M. R. Lyu. Progressive finite newton approach to real-time nonrigid surface detection. In *Computer Vision and Pattern Recognition, 2007. CVPR'07. IEEE Conference on*, pages 1–8. IEEE, 2007.

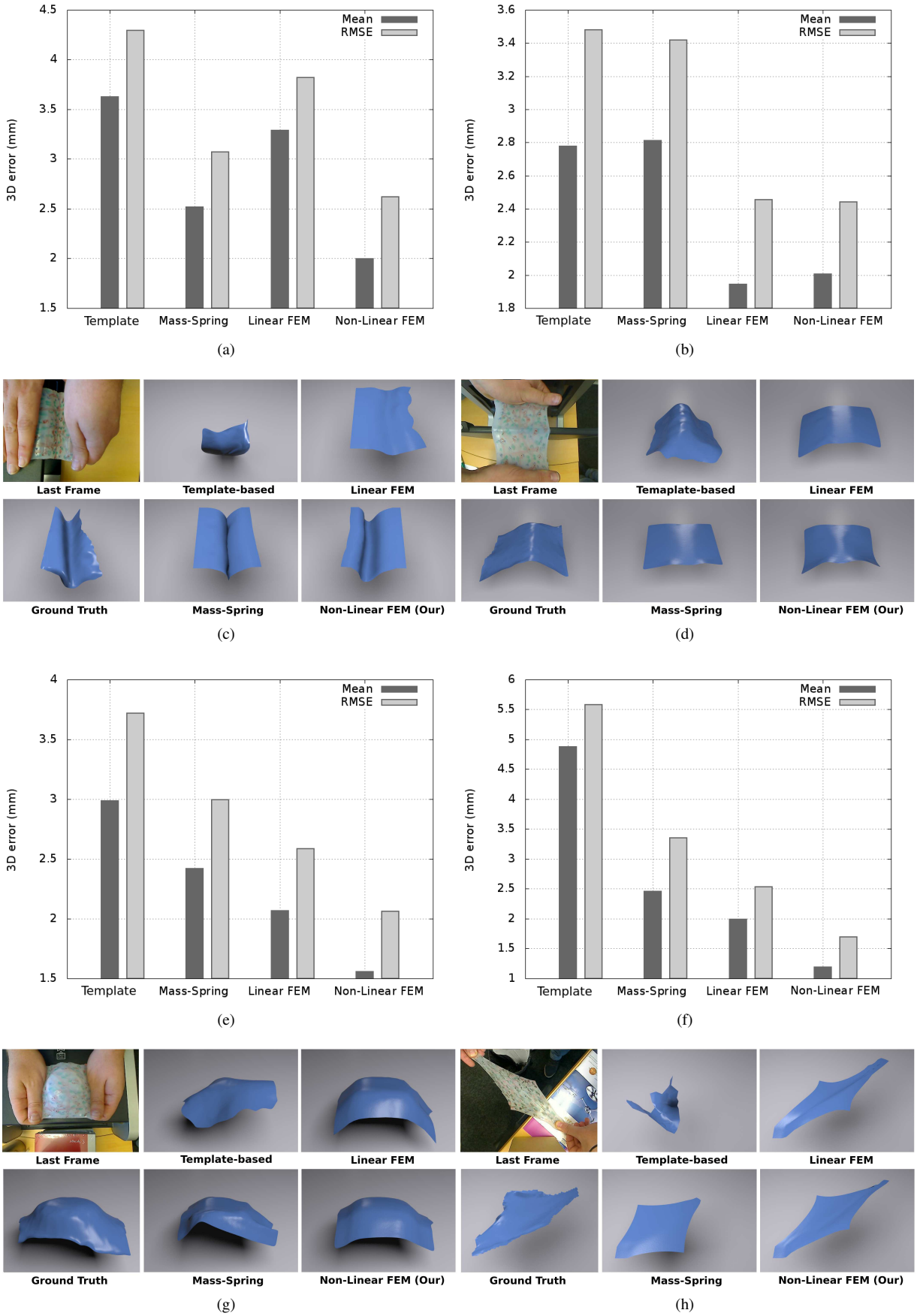

Figure 7: 3D shape recovery of a silicone-like material deformation: Our method produce the lowest error in comparison with other methods on 4 type of deformations and extensibility with (a) and (c) deformation 1, (b) and (d) deformation 2, (e) and (g) deformation 3 and (f) and (h) deformation 4.